Springer

Journal of
Mechanical
Science and
Technology

Journal of Mechanical Science and Technology 23 (2009) 3024~3035

www.springerlink.com/content/1738-494x
DOI 10.1007/s12206-009-0819-0

Modeling and experiments on eddy current damping caused by a permanent magnet in a conductive tube †

Jae-Sung Bae[1,*], Jai-Hyuk Hwang[2], Jung-Sam Park[3] and Dong-Gi Kwag[3]

[1]*Assistant Professor, School of Aerospace and Mechanical Engineering, Korea Aerospace University, Goyang-si, Gyeonggi-do, Korea*

[2]*Professor, School of Aerospace and Mechanical Engineering, Korea Aerospace University, Goyang-si, Gyeonggi-do, Korea*

[3]*Graduate Student, School of Aerospace and Mechanical Engineering, Korea Aerospace University, Goyang-si, Gyeonggi-do, Korea*

(Manuscript received December 5, 2008; Revised March 19, 2009; Accepted July 23, 2009)

Abstract

Eddy currents are induced when a nonmagnetic, conductive material is moving as the result of being subjected to a magnetic field, or if it is placed in a time-varying magnetic field. These currents circulate in the conductive material and are dissipated, causing a repulsive force between the magnet and the conductor. With this concept, eddy current damping can be used as a form of viscous damping. The present study investigates analytically and experimentally the characteristics of eddy current damping when a permanent magnet is placed in a conductive tube. The theoretical model of eddy current damping as the result of a magnet in a copper tube is developed from electromagnetics and is verified from experiments. The experiments include a drop test whereby a magnet is dropped in a copper tube to measure the damping force in a steady-state, and a dynamic test is used to measure the same phenomenon in a dynamic-state. The drop test shows that the present model can accurately predict the force of steady-state damping. From the dynamic test, although predictability is not accurate at high excitation frequencies, the present model can be used to predict damping force at low excitation frequencies.

Keywords: Shock absorber; Vibration suppression; Damping force; Eddy current; Eddy current damping; Electromagnetic damping

1. Introduction

An eddy current is caused when a moving conductor intersects a stationary magnetic field, or vice-versa. The relative motion between the conductor and the magnetic field generates the circulation of the eddy current within the conductor. These circulating eddy currents induce their own magnetic field with the opposite polarity of the applied field that causes a resistive force. These currents dissipate due to the electrical resistance and this force will eventually disappear. Hence, the energy of the dynamic system will be removed. Since the resistive force induced by eddy currents is proportional to the relative velocity, the conductor and the magnet can be allowed to function as a form of viscous damping.

For decades, various applications utilizing eddy currents for damping dynamic systems have been developed, such as in the magnetic braking system [1-4] and the lateral vibration control of rotating machinery [5, 6]. Karnopp [7] introduced a small and light linear electrodynamic motor consisting of copper coils and permanent magnets which can be used as an electromechanical damper for vehicle suspension systems. Larose et al. [8] studied the effectiveness of external means for reducing the oscillations of

† This paper was recommended for publication in revised form by Associate Editor Eung-Soo Shin

* Corresponding author. Tel.: +82 2 300 0102, Fax.: +82 2 3158 3189
E-mail address: jsbae@kau.ac.kr

a full-bridge aeroelastic model using a tuned mass damper (TMD). Their TMD takes advantage of adjustable inherent damping provided by eddy currents. Teshima et al. [9] investigated the effects of an eddy current damper on vibrations associated with superconducting levitation and showed that when eddy current damping was employed, the measured level of vertical vibration improved by approximately a hundredfold.

Additionally, several studies [10-15] have investigated the effects of magnetic fields on vibration in cantilever beams. Takagi et al. [10] studied thin plate deflection in a magnetic field both analytically and through experimentation. Lee [11] studied the dynamic stability of conducting beam plates in a transverse magnetic field and demonstrated the existence of three regions of stability: damped stable oscillation, static asymptotic stability, and static divergence instability. Matsuzaki et al. [12, 13] proposed the concept of a new vibration control system in which the vibration of a partially magnetized beam is suppressed by using electromagnetic forces and performed an experimental study to show the effectiveness of their concept. Recently, Kwak et al. [14] investigated the effects of an eddy current damper (ECD) on a cantilever beam, and their experimental results showed that an ECD can be an effective device for vibration suppression. However, their investigation, while meaningful, failed to produce a detailed eddy current damping model. Bae et al. [15] developed a theoretical model of an ECD constructed by Kwak et al. [14]. Using this theoretical model, the authors investigated the damping characteristics of an ECD and simulated the vibration suppression of a cantilever beam with an attached ECD. Kwak's ECD used the eddy currents induced in the conductive metal which was moving perpendicular to the magnetic poling axis as shown in Fig. 1(a). This concept used the magnet's axial flux induced by two oppositely poled magnets and has been studied by previous researchers [1-4] because of the desirable traits that this method has for magnetic braking. Sodano et al. [16-18] proposed a new concept using the eddy currents induced in a conductive plate which oscillates through the magnetic poling axis as shown in Fig. 1(b). Their concept used the magnet's radial flux induced by using one magnet or two same poled magnets and can be used in the transverse vibration suppression of a cantilever beam.

Kwag et al. [19] proposed and developed the concept of making an eddy current shock absorber using permanent magnets as shown in Fig. 2. The magnetically tuned mass damper developed by CSA Engineering Inc. [20] is similar to this model. However, their model does not require the use of any coil springs because the repulsive force between the magnets takes its place. In their model, permanent magnets are moving in a copper tube and the eddy currents are induced in the tube as shown in Fig. 3. This model also uses the magnet's radial flux as was done

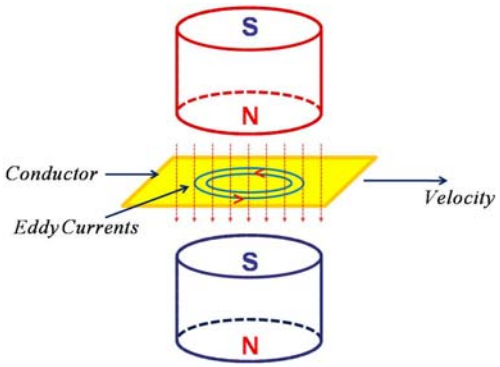

(a) Conductive plate moving perpendicular to the magnetic poling axis

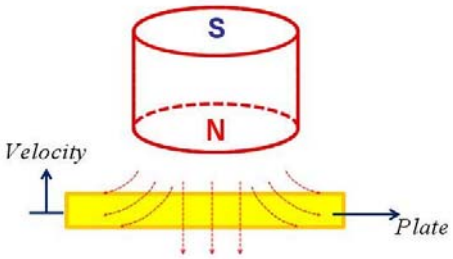

(b) Conductive plate oscillating through the magnetic poling axis

Fig. 1. Concepts of eddy current damping.

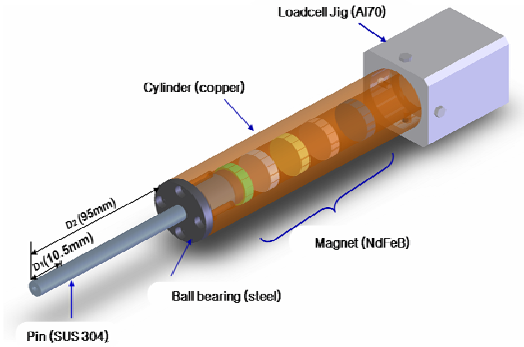

Fig. 2. Eddy current shock absorber by Kwag et al. [19].

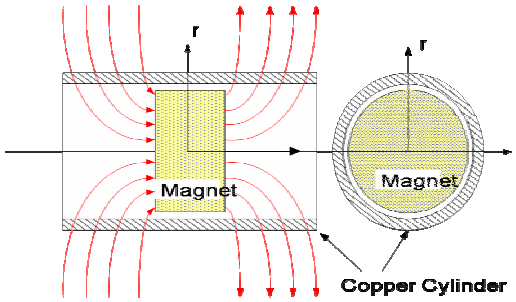

Fig. 3. Permanent magnet in a copper tube.

in Sodano's model, but it is more effective because the radial flux is almost perpendicular to the copper tube surface. As such, using this concept, a shock absorber without coil springs or fluids can be constructed.

The motivation of the present study is to develop and verify a theoretical model of the eddy current damping used by Kwag's eddy current concept. To verify this model, a finite element analysis and associated experiments are performed in order to achieve two interconnected goals. First, the magnetic field which is created by a permanent magnet is calculated, and second, the eddy current damping is accurately measured. The experiments include a drop test and the sinusoidal excitation of a permanent magnet in a copper tube. The former is conducted in order to measure the values of steady-state damping and the latter measures those of dynamic damping. In this way, the characteristics of eddy current damping are investigated analytically and experimentally both in a steady and dynamic state.

2. Theoretical analysis

2.1 Electromagnetic modeling of a permanent magnet

If the surface charges are assumed to be ignored, the current density $\vec{J}$ induced in the conducting sheet moving with the velocity of $\vec{v}$ is given by

$$\vec{J} = \sigma(\vec{v} \times \vec{B}) \tag{1}$$

where σ is the conductivity of the conducting material and the $\vec{v} \times \vec{B}$ term is the electromotive force driving the eddy currents $\vec{J}$.

To calculate magnetic flux density at point $P(R,\theta,z)$, a cylindrical coordinate is used as shown in Fig. 4.

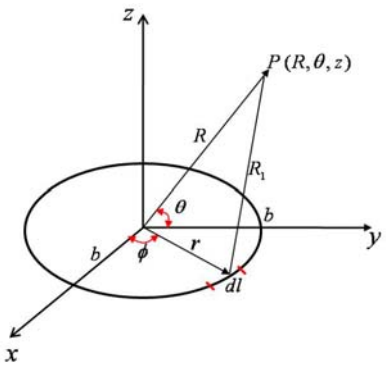

Fig. 4. Schematic of the circular magnetized strip.

Applying the Biot-Savart law to the circular loop shown in Fig. 4, the magnetic flux density can be expressed as

$$d\vec{B} = \frac{\mu_0 M_0}{4\pi} \frac{d\vec{l} \times \hat{R}_1}{R_1^2} \tag{2}$$

where μ_0, M_0, $\hat{R}_1$, and $d\vec{l}$ are the permeability, the magnetization per unit length, the vector from the source point to the field point, and the vector of infinitesimal strip, respectively. The vector $\vec{R}_1$ is defined by the distance between the differential element on the circular strip and the point on the y-z plane as shown in Fig. 4 and written as

$$\vec{R}_1 = \vec{R} - \vec{r} \tag{3}$$

where $\vec{R} = y\vec{a}_y + z\vec{a}_z$ $\vec{r} = b\cos\phi\vec{a}_x + b\sin\phi\vec{a}_y$

The vector $d\vec{l}$ in Eq. (2) can be expressed as

$$d\vec{l} = -b\sin\phi d\phi\vec{a}_x + b\cos\phi d\phi\vec{a}_y \tag{4}$$

where b is the radius of the circular magnet.

Substituting Eqs. (3) and (4) in to Eq. (2), the magnetic flux density due to the circular magnetized strip is

$$dB_y(y,z) = \frac{\mu_0 M_0 bz}{4\pi}\int_0^{2\pi} \frac{\sin\phi}{(b^2+y^2+z^2-2by\sin\phi)^{\frac{3}{2}}} d\phi = \frac{\mu_0 M_0 bz}{4\pi} I_1(b,y,z) \tag{5}$$

$$dB_z(y,z) = \frac{\mu_0 M_0 b}{4\pi}\int_0^{2\pi} \frac{b-y\sin\phi}{(b^2+y^2+z^2-2by\sin\phi)^{\frac{3}{2}}} d\phi = \frac{\mu_0 M_0 b}{4\pi} I_2(b,y,z) \tag{6}$$

where I_1 and I_2 include the elliptic integrals shown in Appendix A. dB_y and dB_z are the magnetic flux density in the direction of y and z, respectively. Hence, the magnetic flux densities due to the circular magnet can be obtained to integrate Eqs. (5) and (6) through the length of magnet and are written as

$$B_y(y,z,z_1)=\frac{\mu_0 M_0 b}{4\pi}\int_{-\frac{h}{2}}^{\frac{h}{2}}(z-z_1)I_1(b,y,z-z_1)dz_1 \quad (7)$$

$$B_z(y,z,z_1)=\frac{\mu_0 M_0 b}{4\pi}\int_{-\frac{h}{2}}^{\frac{h}{2}}I_2(b,y,z-z_1)dz_1 \quad (8)$$

where z_1 and h are the distance in the **z** direction from the center of a magnetized infinitesimal strip and the length of the circular magnet, respectively. The magnetic field distributions in Eqs. (7) and (8) are symmetric about the z-axis.

The electromagnetic force due to the eddy current can be expressed as

$$\vec{F}=\int_V(\vec{J}\times\vec{B})dV \quad (dV=\rho d\rho d\phi dz) \quad (9)$$

When the magnet has the velocity in the z direction, the magnetic flux density $B_z(y,z,z_1)$ does not contribute to the damping force because its cross product with the velocity is zero. Thus, the damping force $\vec{F}_d$ due to the eddy current in the z direction yields

$$\vec{F}_d=v\cdot 2\pi\sigma\delta y\int B^2{}_y(y,z,z_1)dz \quad (-\vec{a}_z) \quad (10)$$

where δ and v are the thickness of copper tube and the vertical velocity of magnet, respectively. From Eq. (10), the eddy current damping coefficient c_d can be defined as

$$c_d=2\pi\sigma\delta y\int B^2{}_y(y,z,z_1)dz \quad (11)$$

Because the analytic integrations of Eqs. (7)-(11) are very difficult, a numerical integration method will be used to obtain the damping coefficient in Eq. (11).

2.2 Terminal speed of a magnet falling in copper tube

To verify the theoretical models in Eqs. (10) and (11), a drop test using a permanent magnet is performed as shown in Fig. 5. When the magnet is released, the magnetic flux in each of the rings begins to change. In accordance with Faraday's Law, this flux change induces an electromotive force and an electric current inside the ring. The magnitude of the current depends on the distance of each ring from the falling magnet and on the magnet's speed. The law of Biot-Savart states that an electric current produces a magnetic field, which, according to Lenz's law, opposes the action that induced it; that is, the emotion of the magnet. Thus, if the magnet is moving away from a given ring, the induced field will attract it, while if it is moving toward a ring, the induced field will repel it. Fig. 5 shows the induced currents above and below the falling magnet. The upper currents attract the magnet whereas the lower currents repel it, thereby yielding the damping force.

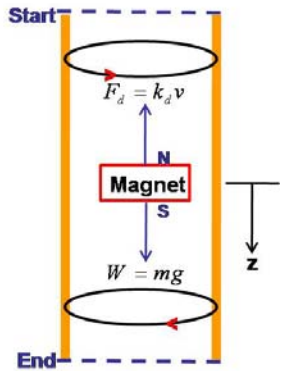

Fig. 5. Free body diagram for a magnet falling.

The net force on the magnet can be calculated by summing the electromagnetic force with all of the rings. The force is an increasing function of the velocity and will decelerate the falling magnet. When the velocity reaches the value at which the magnetic force completely compensates for gravity, the acceleration will be zero and the magnet will fall at a constant terminal speed. For a sufficiently strong magnet, the terminal speed is reached very quickly.

As is well known, the governing equation of a magnet falling in a copper tube is written as

$$W-F_d=mg-c_d v=m\frac{dv}{dt} \quad (12)$$

where c_d (disregarding the aerodynamic friction due to an extremely low speed) and m are the damping coefficient which is associated with the induced current and the mass of the magnet, respectively. Integrating Eq. (12), we obtain

$$v(t)=\frac{mg}{c_d}(1-e^{-\frac{c_d}{m}t}) \quad (13)$$

Thus, integrating Eq. (13), the displacement can be written as

$$x(t) = -\frac{m^2 g}{c_d^{\,2}}(1 - e^{-\frac{c_d}{m}t}) + \frac{mg}{c_d}t \qquad (14)$$

It is observed that the terminal speed (asymptotic speed, mg/c_d) is reached quickly ($m/c_d << 1$). For this reason, we can conclude that through a copper tube length L_c, the falling speed of the magnet can be considered approximately uniform. The predictions of velocity and time to pass out the copper tube can be calculated from Eqs (13) and (14).

3. Numerical and experimental results

3.1 Verification of the magnetic field

The present model of the magnetic field generated by a cylindrical, permanent magnet is verified by referencing the results of a commercial code before estimating the eddy current damping. "Ansoft Maxwell" is a commercial software product designed to analyze magnetic fields. It is the leading electromagnet field simulation software primarily used for the design and analysis of 3D/2D structures, such as motors, actuators, transformers and other electric and electromechanical devices common to the fields of automotive, military/aerospace, and industrial systems. Based on the Finite Element Method (FEM), Maxwell can accurately solve static, frequency-domain and time-varying electromagnetic and electric fields.

As was mentioned in the previous section, only magnetic flux density in the **y** direction can generate damping force. The physical properties of the magnet and copper tube are listed in Table 1.

Table 1. Physical properties of the magnet and copper tube.

Property	Value
Magnet Composition	*NdFeB*35
Magnet Mass	23*g*
Magnet Size	20*10 *mm*
Residual Magnetic Flux Density	1.23*T*
Copper Composition	*pure*
Length of Copper Tube	500 *mm*
External Diameter of Copper Tube	33 *mm*
Internal Diameter of Copper Tube	21*mm*
Thickness of Copper Tube	6 *mm*
Conductivity of Copper Tube	$5.8\times10^7\ S/m$

After applying these properties to the Maxwell program, the magnetic flux can be obtained. The contours of the magnitude of magnetic flux density in the **y-z** surface of the copper tube are shown in Fig. 6. This Fig. shows that the magnet has a stronger magnetic flux density at the corner of the magnet. This phenomenon is reasonable because most of the magnetic flux density is turned downward at a corner. Fig. 7 shows the variation of the magnetic flux density B_y of the center of a copper tube. As shown, the maximum value of the radial magnetic flux density B_y is observed at the boundary of the magnet, and the magnetic flux density subsequently becomes approximately zero as the distance is greater than 20mm from the magnetic surface. This Fig. also shows that the results of the present model and those from the Maxwell simulation match up well. Thus, the present model of the magnetic field is assumed to be very accurate, and a detailed description of an experiment with eddy current damping in a steady state can now follow.

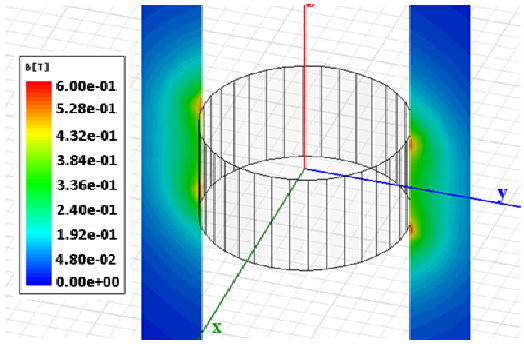

Fig. 6. Magnitude B (T) on copper in y-z plane.

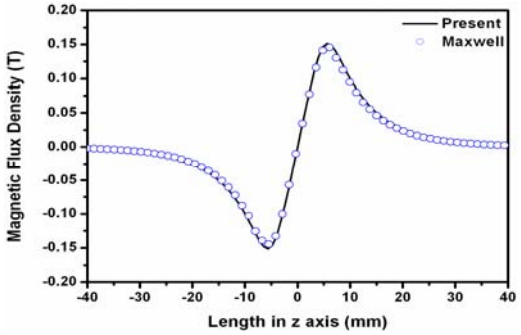

Fig. 7. Comparison between the present model and Maxwell software.

3.2 Eddy current damping in a steady state

To validate the accuracy of the present model, a drop test of a magnet in a copper tube is performed. This experiment is conducted in order to estimate the eddy current damping in a steady state. "Steady state" means that the eddy current damping force is not a function of time. At the terminal speed, the damping force is constant because the dropping magnet is in equilibrium between gravitational force and the drag force.

A Neodymium-Iron-Boron permanent magnet and a pure copper cylinder are used for this experiment. Using Eqs. (13) and (14), the displacement and velocity of the falling magnet in the tube can be calculated as shown in Fig. 8. The terminal speed of the magnet is about 22.09 mm/s. Since the time to reach the terminal speed is short, the terminal speed can be assumed to be the average velocity. Thus, the terminal speed of the drop test is calculated from the measured time to reach the tube end and the tube length.

Table 2. Comparison between prediction and experiment.

Terminal speed		Damping Coefficient	
Prediction	Experiment	Prediction	Experiment
22.09 mm/s	20.45 mm/s	10.290 kg/s	11.021 kg/s

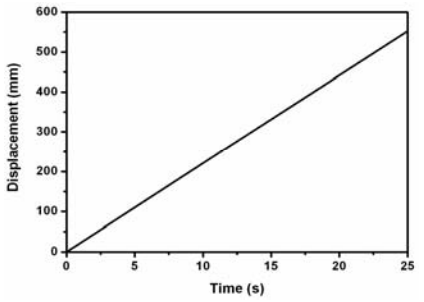

(a) Displacement

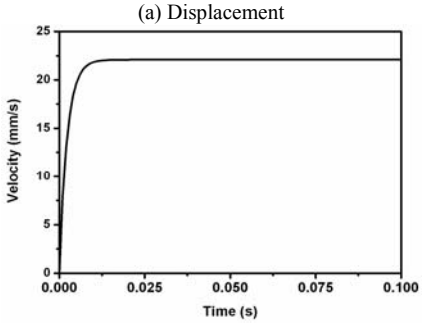

(b) Velocity

Fig. 8. Displacement and velocity of the magnet falling in the tube.

Table 2 shows the comparison between the present predictions and the experimental results. The predictions and experimental results are within acceptable parameters in terms of terminal speed and the damping coefficient. The small discrepancies between the predictions and the actual experiment are assumed to be a result of the surface friction and aerodynamic damping when the magnet passes through a cylindrical copper tube. Thus, the present model is sufficiently accurate for predicting steady-state eddy current damping. The following section will discuss the dynamic characteristics of eddy current damping.

3.3 Dynamic characteristics of an eddy current damping

To investigate the dynamic characteristics of dynamic eddy current damping, an experimental apparatus is set up as shown in Fig. 9. The energy created by the rotational motion of a DC motor is transferred to the rectilinear movement of a rod by the cam. The rod pushes and pulls the permanent magnet in the conducting cylinder (Fig. 10). The electromagnetic force and the displacement of the magnet are measured by a load cell and a laser displacement sensor, respectively.

The motion is expressed as

$$x(t) = A\sin(2\pi f_n t) \tag{15}$$

where, A and f_n are the amplitude and excitation

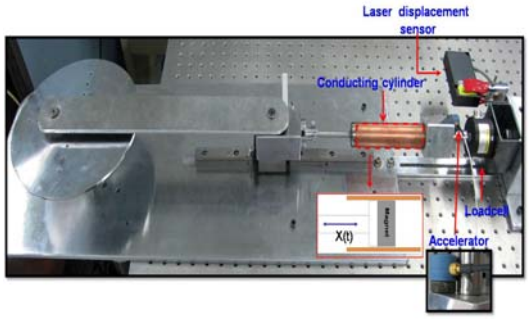

Fig. 9. Experimental setup for a dynamic test.

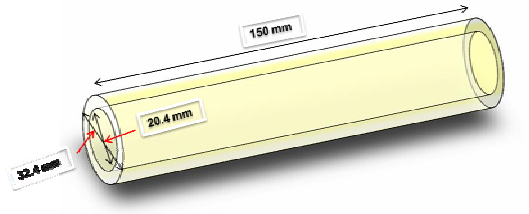

Fig. 10. Conductive cylinder for a dynamic experiment.

frequency, respectively.

The time signals of displacement, velocity and force are shown in Fig. 11 when the amplitude is 20 *mm* and the excitation frequencies are 1.0 Hz and 2.0 Hz, respectively. The velocity signal is obtained by differentiating the displacement. The noise of these signals is so small that it can be ignored in the dynamic test. The measured force signal may include undefined forces like friction between the magnet and cylinder. To measure these forces, the same experiment is performed using a plastic cylinder instead of a magnet. These forces are eliminated from the measured force signal and it is assumed that the force signal in Fig. 11 represents only the eddy current damping force. Fig. 11 shows that the velocity and force signals have the same phase angles with respect to displacement. Based on the eddy current theory in Eq. (10), the eddy current damping force is proportional to the velocity. Hence, it can be concluded that the experimental setup in Fig. 9 is working well and can be used to perform the dynamic test of eddy current damping.

Using this experimental setup, the dynamic test was performed for various excitation frequencies. Figs. 12 and 13 show the force-displacement plots and the force-velocity plots at several frequencies. The plots of Fig. 12 have hysteresis loops. The hysteresis loop is a typical phenomenon that occurs with viscous damping, and the area encapsulated by the loop indicates the energy dissipation that is caused by eddy current damping. These results show that eddy current damping can be used as a shock absorber in vibrating systems. The plots of Fig. 13 also have hysteresis loops, and this result indicates that there is a spring force. The slopes of Figs. 12 and 13 indicate the spring coefficients and damping coefficients, respectively. From the results of Figs. 12 and 13, these coefficients can be estimated by system identification [21]. Table 3 shows the maximum velocity, spring coefficient, damping coefficient, and maximum damping force. As the excitation frequency increases, the spring constant increases, but the damping coefficient decreases. Although the damping coefficient decreases, the maximum damping force increases because the maximum velocity increases. The steady-state damping coefficient predicted from Eq. (11) is 12.21 kg/s. Based on this value, it can be concluded that the present model accurately predicts eddy current damping at low excitation frequencies. However, at high excitation frequencies, over 5.0 Hz, the difference between the predictions and experimental results is too large.

Table 3. Spring coefficients, damping coefficients, and maximum damping forces.

Parameter	Spring coefficient (N/m)	Damping coefficient (kg/s)	Maximum damping force (N)
$A=20mm \quad f=1.0Hz$	26.10	13.49	2.10
$A=20mm \quad f=1.5Hz$	34.62	13.06	2.43
$A=20mm \quad f=2.0Hz$	53.93	12.63	3.28
$A=20mm \quad f=3.0Hz$	104.39	10.05	4.28
$A=20mm \quad f=4.0Hz$	135.87	9.30	5.47
$A=20mm \quad f=6.0Hz$	230.62	6.95	7.16
$A=20mm \quad f=8.0Hz$	285.48	5.39	8.10

Fig. 14 shows damping coefficients and forces in relation to velocity. The predictions and experimental results for both the damping coefficient and force

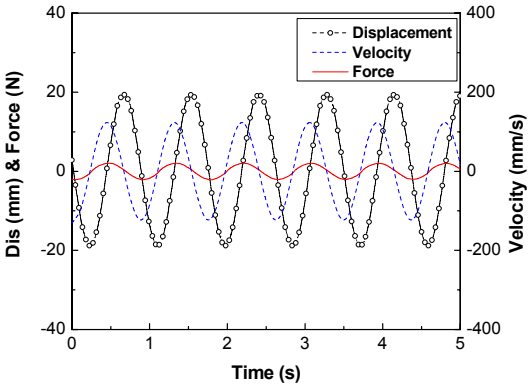

(a) $A=20mm \quad f_n=1.0\ Hz$

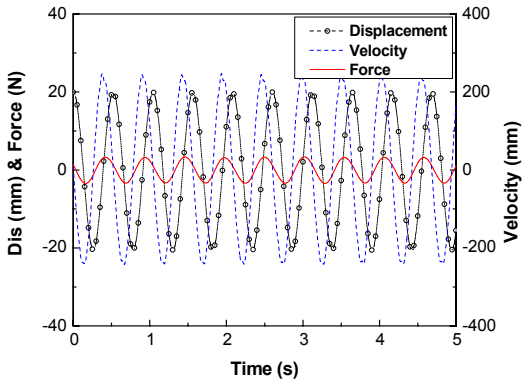

(b) $A=20mm \quad f_n=2.0\ Hz$

Fig. 11. Time histories of displacement, velocity and damping force.

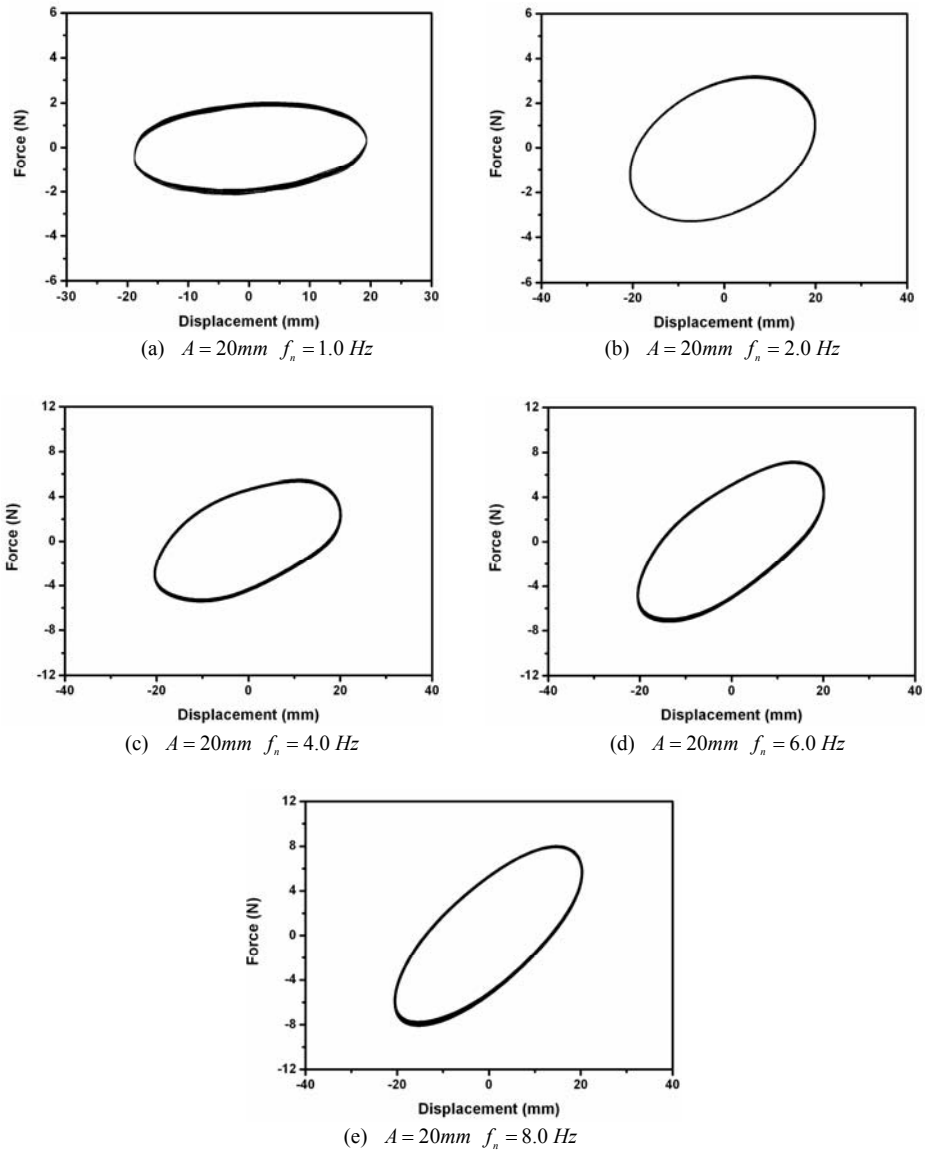

(a) $A = 20mm \;\; f_n = 1.0\ Hz$ (b) $A = 20mm \;\; f_n = 2.0\ Hz$

(c) $A = 20mm \;\; f_n = 4.0\ Hz$ (d) $A = 20mm \;\; f_n = 6.0\ Hz$

(e) $A = 20mm \;\; f_n = 8.0\ Hz$

Fig. 12. Force – Displacement plots for various frequencies.

match up well when a velocity is about 120-500 mm/s. This velocity region is 1.0-4.0Hz. Although small differentiation occurs, the damping coefficients within this region are approximately constant. Over about 300 mm/s, the damping coefficient decreases. The slope of the damping force changes at this velocity. The dynamic results in Figs. 12-14 reveal that the ability of eddy current damping decreases as the sinusoidal excitation frequency increases.

From Eqs. (10) and (11), it is apparent that only the damping force is present. However, the experimental results in Fig. 12 show that a spring force component exists. Although the predictions agree well with experiments at the low excitation frequency, especially under about 4 Hz, the predictions do not at the high excitation frequency. The present eddy current model was derived from the assumption that an electrostatic condition would prevail, meaning that the magnetic fields would be time-invariant. This assumption does in fact hold true during the magnet drop test because its velocity is constant and the eddy current is in a steady state.

When the magnet is excited by sinusoidal motion the velocity is no longer constant and the eddy current

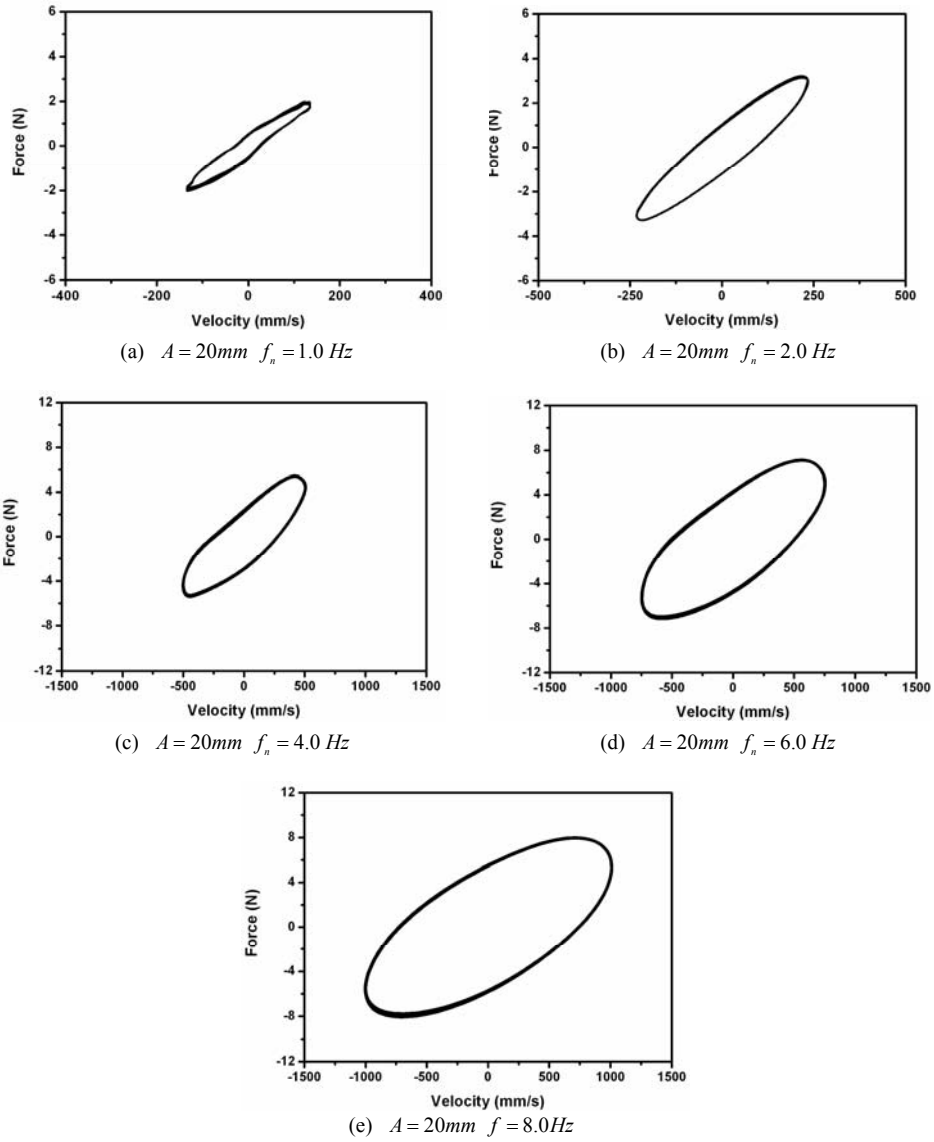

Fig. 13. Force–velocity plots for various frequencies.

damping becomes time-variant. As mentioned, the eddy currents are induced in the copper tube due to the time-varying magnetic field. These currents induce the magnetic field by Ampere's law and then the net magnetic field is eventually decreased. This induced magnetic field was ignored in the derivation of the present model. The assumption of ignoring the induced magnetic field can stand for the drop test because the induced eddy currents become more distant and dissipate by heat. Thus, the effects of the induced magnetic field can be ignored. However, since the magnet moves back to the eddy currents for the harmonic excitation the induced magnetic field becomes important and cannot be ignored. At the low excitation frequency this effect becomes less important because the magnet moves back slowly and the currents dissipate. For these reasons, the present and experimental results do not agree well at high excitation frequencies. Yet, it is important to note that although the present eddy current damping model does not perform well at the high excitation frequency, the model still has considerable merit in that it provides consistently accurate predictions for the drop test and the harmonic excitation of low frequencies.

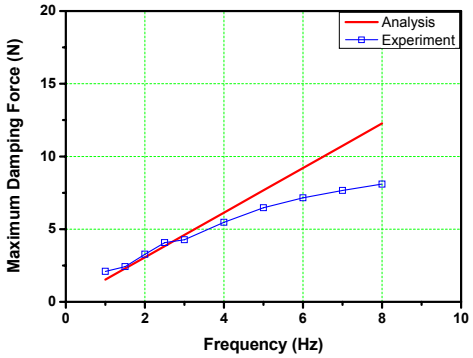

Fig. 14. Predictions and experiment results.

4. Conclusions

The present study has introduced a new concept of eddy current damping using a magnet in a copper tube. The advantage of eddy current damping is primarily its simplicity; this method of damping requires neither fluid nor energy. Based on the steady-state assumption and electromagnetics, the theoretical model depicted above was derived by making possible an electromagnetic damping force induced on a copper cylinder. The experiments were performed to verify the utility of the theoretical model and included a drop test and dynamic test of a permanent magnet in a copper tube. The drop test and dynamic test were chosen as proxies for steady damping and dynamic damping, respectively.

The drop test indicates that the present model is remarkably accurate for steady damping. Results from the dynamic test were more mixed. When high excitation frequencies were encountered, the predictions created by the model did not correlate well with the figures produced by the actual experiment. However, the predictions were sufficiently accurate when the excitation frequencies were low, especially under about 4 Hz. Given that an accurate eddy current model is necessary to provide accurate predictions regarding damping, the model presented here is of considerable value. It is expected that this conception of eddy current damping can be used with the development of shock absorbers. In particular, the present eddy current damping model can be used to estimate the eddy current damping accurately if the right conditions are present.

Acknowledgments

This work was supported by the Agency for Defense Development (ADD) in Korea, and this support is gratefully acknowledged.

Nomenclature

b	:	Radius of magnet
J	:	Current density
B	:	Magnetic flux density
v	:	Velocity of magnet
h	:	Thickness of magnet
c_d	:	Damping coefficient
μ_0	:	Permeability
F_d	:	Damping force
σ	:	Conductivity of copper
r	:	Temporal coordinate
L_c	:	Length of copper tube
ϕ	:	Assumed mode shaped
δ	:	Thickness of copper tube
V	:	Volume
M_0	:	Magnetization
t	:	Time

References

[1] H. H. Wiederick, N. Gauthier and D. A. Campbell, Magnetic braking: Simple Theory and Experiment, *Am. J. Phys.* 55 (1987) 500-503.

[2] M. A. Heald, Magnetic Braking: Improved Theory, *Am. J. Phys.* 56 (1988) 521-522.

[3] L. H. Cadwell, Magnetic Damping: Analysis of an Eddy Current Brake using an Airtrack, *Am. J. Phys.* 64 (1996) 917-923.

[4] K. J. Lee and K. J. Park, A Contactless Eddy Current Brake System, *IEEE Conf. on Intelligent Processing Systems*, Australia. Dec. (1998) 193-197.

[5] G. Genta, C. Delprete, A. Tonoli, E. Rava and L. Mazzocchetti, Analytical and Experimental Investigation of a Magnetic Radial Passive Damper, *Proc. of the Third International Symposium on Magnetic Bearings*. (1992) 255-264.

[6] Y. Kligerman, A. Grushkevich, M. S. Darlow and A. Zuckerberger, Analysis and Experimental Evaluation of Inherent Instability in Electromagnetic Eddy-Current Damper Intended for Reducing Lateral Vibration of Rotating Machinery, *Proc of ASME: 15th Biennial Conference on Vibration and Noise*, Boston, MA. (1995) 1301-1309.

[7] D. Karnopp, Permanent Magnet Linear Motors Used as Variable Mechanical Damper for Vehicle Suspensions, *Veh. Syst. Dynam.* 18 (1989) 187-200.

[8] G. L. Larose, A. Larsen and E. Svensson, Modeling of Tuned Mass Dampers for Wind-tunnel Tests on a Full-bridge Aeroelastic Model, *J. W. Eng. Indust. Aerodynam.* 54/55 (1995) 427-437.

[9] H. Teshima, M. Tanaka, K. Miyamoto, K. Nohguchi and K. Hinata, Effect of Eddy Current Dampers on the Vibrational Properties in Superconducting Levitation using Melt-processed YbaCuO bulk Superconductors, *Physic C*. 274 (1997) 17-23.

[10] T. Takagi, J. Tani, S. Matsuda, S. Kawamura, Analysis and Experiment of Dynamic Deflection of a Thin Plate with a Coupling Effect, *IEEE Trans. Magn.* 28 (1992) 1259-1262.

[11] J. S. Lee, Dynamic Stability of Beam Plates in Transverse Magnetic Fields, *J. Eng. Mecha.* 122 (1996) 89-94.

[12] Y. Matsuzaki, Y. Ishikubo, T. Kamita and T. Ikeda, Vibration Control System Using Electromagnetic Forces, *J. Intell. Mater. Syst. Struct.* 8 (1997) 751-756.

[13] Y. Matsuzaki, T. Ikeda, A. Nae and T. Sasaki, Electromagnetic Forces for a New Vibration Control System: Experimental Verification, *Smart. Mater. Struct.* 9 (2000) 127-131.

[14] M. K. Kwak, M. I. Lee and S. Heo, Vibration Suppression Using Eddy Current Damper, *K. S. N. V. E.* 233 (2003) 441-453.

[15] J. S. Bae, M. K. Kwak and D. J. Inman, Vibration Suppression of Cantilever Beam Using Eddy Current Damper, *J. S. V*. 284 (2005) 805-824.

[16] H. A. Sodano, J. S. Bae, D. J. Inman and W. K. Belvin, Concept and Model of Eddy Current Damper for Vibration Suppression of a Beam, *J. S. V*. 288 (2005) 1177-1196.

[17] H. A. Sodano, J. S. Bae, D. J. Inman and W. K. Belvin, Modeling and Application of Eddy Current Damper for Suppression of Membrane Vibration, *AIAA Journal*. 44 (2006) 541-548.

[18] H. A. Sodano, J. S. Bae, D. J. Inman and W. K. Belvin, Improved Concept and Model of Eddy Current Damper, *J. Vib. Acous.* 128 (2006) 294-302.

[19] D. G. Kwag, J. S. Bae and J. H. Hwang, Experimental Study for Dynamic Characteristics of an Eddy Current Shock Absorber, *J. KSAS.* 35 (2007) 1089-1094.

[20] CSA Engineering Inc., http://www.csaengineering.com.

[21] D. K. Kim, J. S. Bae, I. Lee and J. H. Han, Dynamic Model Establishment of a Deployable Missile Control Fin with Nonlinear Hinge, *J. Spacecraft. Rockets.* 42 (2005) 66-76.

Appendix-Integrals defining the magnetic flux density

The integration I_1 in Eq. (5) is

$$I_1(b,y,z)=\int_0^{2\pi}\frac{\sin\phi}{(b^2+y^2+z^2-2by\sin\phi)^{\frac{3}{2}}}d\phi$$
$$=\frac{1}{bynp^2}[m^2\{E_1(\frac{\pi}{4},-\frac{4yb}{n^2})+E_1(\frac{3\pi}{4},-\frac{4yb}{n^2})\}$$
$$-p^2\{E_2(\frac{\pi}{4},-\frac{4yb}{n^2})+E_2(\frac{3\pi}{4},-\frac{4yb}{n^2})\}] \quad (A.1)$$

where

$$m^2=b^2+y^2+z^2,\ \ n^2=(b-y)^2+z^2,$$
$$p=(b+y)^2+z^2 \quad (A.2\text{-}A.4)$$

The elliptic integrals of Eq. (A.1) are

$$E_1=(\phi,m)=\int_0^{\phi}(1-m\sin^2\theta)^{1/2}d\theta \quad (A.5)$$

$$E_2=(\phi,m)=\int_0^{\phi}(1-m\sin^2\theta)^{-1/2}d\theta \quad (A.6)$$

The integration I_2 in Eq. (6) is

$$I_2(b,y,z)=\int_0^{2\pi}\frac{b-y\sin\phi}{(b^2+y^2+z^2-2by\sin\phi)^{\frac{3}{2}}}d\phi$$
$$=\frac{1}{bnp^2}[s\{E_1(\frac{\pi}{4},-\frac{4yb}{n^2})+E_1(\frac{3\pi}{4},-\frac{4yb}{n^2})\}$$
$$+p^2\{E_2(\frac{\pi}{4},-\frac{4yb}{n^2})+E_2(\frac{3\pi}{4},-\frac{4yb}{n^2})\}] \quad (A.7)$$

$$s=b^2-y^2-z^2,\ \ n^2=(b-y)^2+z^2,$$
$$p=(b+y)^2+z^2 \quad (A.8\text{-}A.9)$$

The elliptic integrals of Eq. (A.7) are

$$E_1=(\phi,m)=\int_0^{\phi}(1-m\sin^2\theta)^{1/2}d\theta \quad (A.10)$$

$$E_2=(\phi,m)=\int_0^{\phi}(1-m\sin^2\theta)^{-1/2}d\theta \quad (A.11)$$

Jae-Sung Bae received his B.S. degree in Aeronautical and Mechanical Engineering from Korea Aerospace University in 1996 and his M.S. degree in Aerospace Engineering from KAIST in 1998. He then received his Ph.D. in Aerospace Engineering from KAIST in 2002. Dr. Bae is currently an Assistant Professor at the School of Aerospace and Mechanical Engineering at Korea Aerospace University in Goyang-City, Korea. His main research interests include aeroelasticity, vibration and control, shock absorber, and recoil system.